

## Supplementary Data

### **Photoelectrode/Electrolyte interfacial band lineup engineering with alloyed III-V thin films grown on Si substrate.**

*Mekan Piriye<sup>a</sup>, Gabriel Loget<sup>b</sup>, Yoan Léger<sup>a</sup>, Hanh Vi Le<sup>c</sup>, Lipin Chen<sup>a, c</sup>, Antoine Létoublon<sup>a</sup>, Tony Rohel<sup>a</sup>, Christophe Levallois<sup>a</sup>, Julie Le Pouliquen<sup>a</sup>, Bruno Fabre<sup>b</sup>, Nicolas Bertru<sup>a,\*</sup>, Charles Cornet<sup>a,\*</sup>*

*<sup>a</sup>Univ Rennes, INSA Rennes, CNRS, Institut FOTON – UMR 6082, F-35000Rennes, France*

*<sup>b</sup>Univ Rennes, CNRS, ISCR (Institut des Sciences Chimiques de Rennes)–UMR6226, F-35000 Rennes, France*

*<sup>c</sup>Tianjin Key Laboratory of Film, Electronic and Communication Devices, School of Integrated Circuit Science and Engineering, Tianjin University of Technology, Tianjin 300384, China*

*Corresponding authors: [charles.cornet@insa-rennes.fr](mailto:charles.cornet@insa-rennes.fr), [nicolas.bertru@insa-rennes.fr](mailto:nicolas.bertru@insa-rennes.fr)*

## Experimental section

**Materials:** GaP<sub>1-x</sub>As<sub>x</sub> alloys with various arsenic content, were epitaxially grown on (001) silicon substrates (Sil'tronix Silicon Technologies), misoriented 6° off toward [110], 350 ± 30 μm thick, n-type doped with phosphorus and with a resistivity of 5-10 Ohm·cm. The reference samples were commercial GaAs and GaP wafers (Wafer Technology Ltd.) n-doped with silicon (1 to 5 × 10<sup>18</sup> cm<sup>-3</sup>), one side polished, and with a thickness of 350 ± 25 μm. For the photoelectrochemical (PEC) characterizations, sulfuric acid (96% H<sub>2</sub>SO<sub>4</sub> VLSI grade Selectipur) diluted with the ultrapure water with a resistivity of 18.2 MΩ·cm (Purelab Classic UV from Veolia Water STI) was used as electrolyte solution.

**Silicon substrate preparation for epitaxy:** Before GaP<sub>1-x</sub>As<sub>x</sub> layer growths, Si substrates were dipped in HF (1%) for 90 seconds, followed by ultraviolet-ozone (UV-O<sub>3</sub>) surface treatment for 5 minutes. The process is repeated 3 times. At final step, silicon substrate was dipped in HF, in order to produce a hydrogen passivated surface.

**MBE growth of GaP<sub>1-x</sub>As<sub>x</sub>:** The HF-chemically prepared substrate was heated up to 800°C for 10 min to desorb hydrogen. A detailed description for the pre-growth preparation of the substrate can be found elsewhere.<sup>1</sup> Then, 1 μm-thick GaP<sub>1-x</sub>As<sub>x</sub> layers were epitaxially grown at 500 °C, at 0.24 ML/s in conventional Molecular Beam Epitaxy (MBE) conditions. The control of the alloy composition was ensured by varying the relative fluxes of As and P, as commonly performed in MBE. Table S 1 summarizes the main growth parameters. It should be noted that the GaP<sub>1-x</sub>As<sub>x</sub> epilayer was not intentionally doped, and epitaxial strategies to annihilate antiphase boundaries (APBs) were not used, leading to the presence of emerging APBs.<sup>2</sup>

	GaP <sub>1-x</sub> As <sub>x</sub> alloys				
<b>x(As)</b>	<b>1</b>	<b>0.83</b>	<b>0.52</b>	<b>0.22</b>	<b>0</b>
V/III ratio	7.4	5.7	5.1	3.9	8.7
Epilayer Thickness (μm)	1	1	1	1	1
MBE growth rate (ML/s)	0.24	0.24	0.24	0.24	0.24

*Table S 1. Growth parameters used for the epitaxy of GaP<sub>1-x</sub>As<sub>x</sub> alloys on Si substrate with the As content x(As), Beam Equivalent Pressure V/III ratio, epilayer thickness and MBE growth rate.*

## Characterizations

**X-Ray Diffraction (XRD):** The structural characterization of the epitaxial GaP<sub>1-x</sub>As<sub>x</sub> alloys was carried out using X-ray Smartlab Rigaku diffractometer (sealed tube Cu source). A parabolic multilayer mirror and a 2 bounce Ge (220) monochromator were used for beam definition and monochromatization. The detection was ensured by a Hypixis 3000 detector working either in 1D mode for reciprocal space maps (RSM) or 0D mode for line scans.

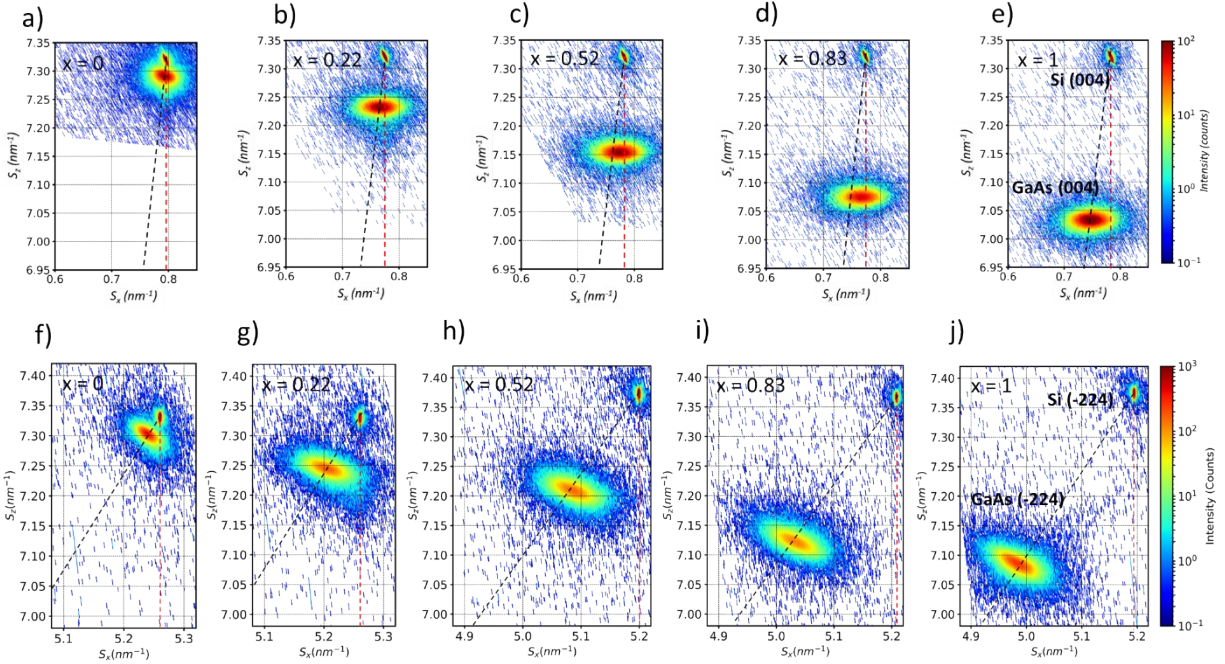


Figure S 1. Reciprocal Space Maps (RSM) showing the Si substrate and the epilayer Bragg peaks around the (004) (a-e) and (-224) crystallographic orientations (f-j). The black and red dashed lines represent the fully plastically relaxed and fully elastically strained lines, respectively.  $x$  refers to the composition  $x(\text{As})$  of  $\text{GaP}_{1-x}\text{As}_x/\text{Si}$  alloys.

**Atomic Force Microscopy (AFM):** The measurements were performed with a Veeco Innova AFM microscope. A contact mode was used with a cantilever set-point fixed at -0.35 V. The measured surface area was  $5 \times 5 \mu\text{m}^2$ . The rms (root-mean-square) roughness was calculated for the whole  $5 \times 5 \mu\text{m}^2$  area and represented in the inset of Figure 2 in the main file.

**Scanning Electron Microscopy (SEM):** The measurements were carried out using a JEOL JSM-7100 scanning electron microscope. The side-view images of the two  $\text{GaP}_{1-x}\text{As}_x$  alloys with a high roughness  $x(\text{As}) = 1$  (Figure S 2a) and a low roughness  $x(\text{As}) = 0.5$  (Figure S 2d) show clearly the Si substrate and the 1- $\mu\text{m}$  thick epilayer, confirming the targeted thickness of the epilayer. The difference in roughness can be observed from the tilted-top view SEM images, as also evidenced

by AFM. SEM images taken from the top view for  $x(\text{As})=1$  epilayer (Figure S 2c) and a commercial GaAs wafer (Figure S 2f) reveals a higher roughness for the epitaxial sample, which is related to the presence of emerging defects.

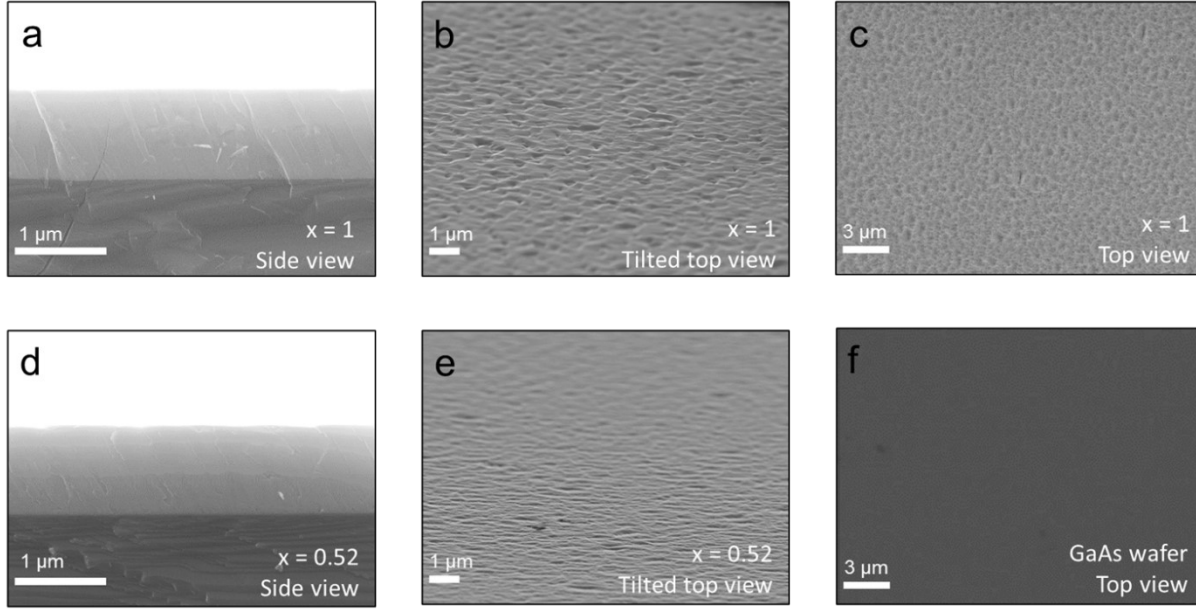


Figure S 2. SEM images for the 1  $\mu\text{m}$ -thick epitaxial  $\text{GaP}_{1-x}\text{As}_x$  alloy grown on Si with high roughness ( $x(\text{As})=1$ ): side view (a), tilted top view (b) and top view (c); low roughness ( $x(\text{As})=0.52$ ): side view (d) and tilted top view (e). Top-view SEM picture of a commercial GaAs wafer (f).

**Spectroscopic ellipsometry:** A Horiba UVISSEL2 spectroscopic ellipsometer was used to measure the optical parameters of epitaxial  $\text{GaP}_{1-x}\text{As}_x$  alloys grown on Si substrate. The ellipsometer parameters were measured at room temperature between 0.6 and 4.2 eV photon energy and then fitted with Tauc-Lorentz model to extract the band gap ( $E_G$ ), the absorption coefficient ( $\alpha$ ), the thickness and the roughness. Table S 2 shows parameters extracted from the fitting of ellipsometry data. Extracted values for the roughness are very similar to those determined by AFM, values of

thickness slightly lower than the targeted one (1  $\mu\text{m}$ ) are obtained, due to ellipsometry fitting uncertainties.

$x(\text{As})$	Alloys				
	<b>1</b>	<b>0.83</b>	<b>0.52</b>	<b>0.22</b>	<b>0</b>
$E_G$ (eV)	1.39	1.46	1.81	2.18	2.41
Thickness ( $\mu\text{m}$ )	0.942	0.816	0.836	0.866	0.722
Roughness ( $\mu\text{m}$ )	0.011	0.017	0.009	0.013	0.011

Table S 2. Extracted band gap, thickness and roughness from the fitting of the ellipsometry data.

The raw ellipsometry data for the  $\text{GaP}_{1-x}\text{As}_x$  sample with  $x(\text{As})=0.5$  and the corresponding Tauc-Lorentz fitting are plotted in Figure S 3a.  $I_s$  and  $I_c$  are related to ellipsometry variables  $\psi$  (amplitude component) and  $\Delta$  (phase difference) through the following equations:  $I_s = \sin(2\psi) \times \sin(\Delta)$  and  $I_c = \sin(2\psi) \times \cos(\Delta)$ . The black lines correspond to the fitting curves with a Tauc-Lorentz model.

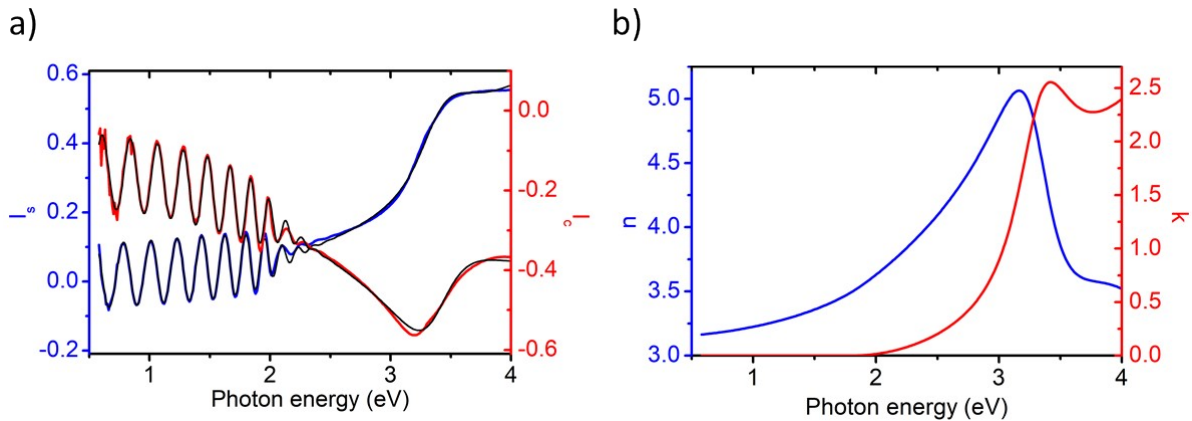


Figure S 3. Raw ellipsometry data showing the variation of  $I_s$  and  $I_c$  parameters and Tauc-Lorentz 2 model fitting (a). Extracted real and imaginary parts of the optical index (b).

Figure 3b shows the  $n$  and  $k$  optical constants deduced from the Tauc-Lorentz fit. The imaginary part of the refractive index ( $k$ ) is used to calculate the absorption coefficient ( $\alpha$ ) through the following equation,  $\alpha = 4\pi k/\lambda$ . The absorption coefficients of  $\text{GaP}_{1-x}\text{As}_x$  alloys are plotted in Figure

S 4.  $\alpha$  values for GaAs and GaP wafers, calculated using optical constants from reference <sup>3</sup>, are also plotted.

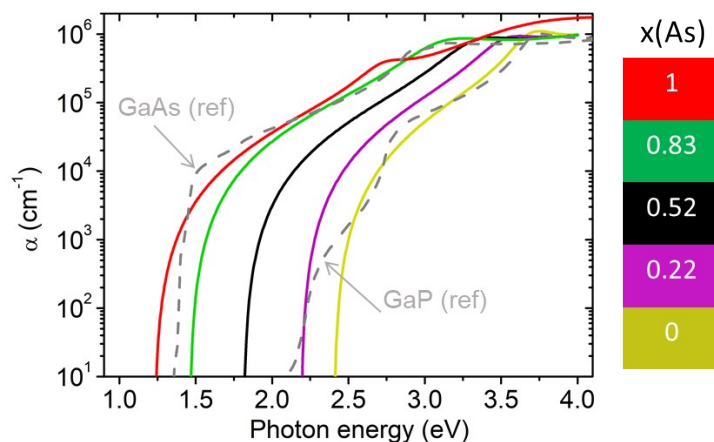


Figure S 4. Measured absorption spectra for the epitaxial  $\text{GaP}_{1-x}\text{As}_x$  alloys grown on Si substrate, including bare GaP and GaAs references for comparison.

**Incident photon-to-current conversion efficiency (IPCE):** IPCE measurements were performed with a CIMPS-QE IPCE 3 workstation (Zahner) comprising a TLS03 tunable light source with the photon energy range of (1.2 – 4.2) eV. The measurements were carried out using a standard three-electrode PEC cell, consisting of a working electrode, a reference electrode (Ag/AgCl in saturated KCl), and a counter electrode (graphite rod), all are connected through an electrochemical potentiostat (Zahner-Zennium). The applied potential was 1 V vs RHE. The set up parameters were: light modulation frequency: 1 Hz, settling time: 5 s, and number of counts equal to 25. For comparison, the IPCE spectrum of the commercial GaAs wafer was recorded as well.

**Flat-band potential ( $V_{fb}$ ):** Mott-Schottky  $1/C_{sc}^2 - E$  (with  $C_{sc}$ , the space-charge capacitance) measurements were performed in the dark in the range of -1.2 V to 0.4 V vs RHE with an AC amplitude of 5 mV and a frequency of 1kHz. Figure S 5 displays the Mott-Schottky plots for  $GaP_{1-x}As_x$  alloys. Further, the flat band potential ( $V_{fb}$ ) is deduced from the Mott-Schottky equation (eq.1) written below.

$$\frac{1}{C_{SC}^2} = \frac{2}{eN_D A^2 \epsilon_0 \epsilon_r} \left( V - V_{fb} - \frac{kT}{e} \right) \quad (1)$$

Where,  $\epsilon_r$  is the relative semiconductor permittivity,  $\epsilon_0$  is the vacuum permittivity,  $A$  the surface area,  $e$  is the electron charge,  $N_D$  is the free carrier density,  $k$  is Boltzmann constant,  $T$  is the temperature,  $V$  is the applied potential. The  $V_{fb}$  can be extracted from the x-intercept of the  $1/C_{sc}^2$  (y-axis) of the linear portion of the MS plot.<sup>5</sup>

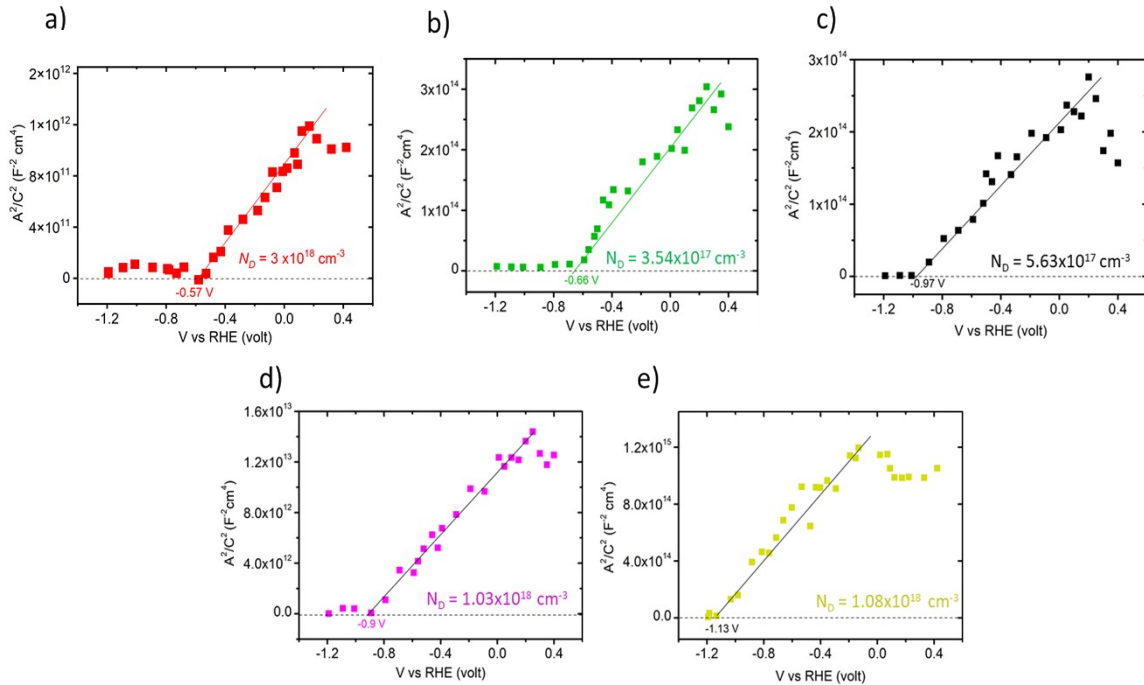


Figure S 5. Mott-Schottky plots performed in the dark for  $GaP_{1-x}As_x$  alloys with different  $x(As)$ : 1 (a), 0.83 (b), 0.52(c), 0.22(d) and 0 (e). Electrolytic solution: 0.2M  $H_2SO_4$  (pH = 0.35).



**Linear sweep voltammetry (LSV):** The photocurrent density ( $j$ ) versus voltage ( $V$ ) measurements were performed in the same three-electrode PEC cell as that used for the IPCE measurements. The illumination was provided by a solar simulator (LS0106, LOT Quantum Design) equipped with an AM 1.5G filter providing a stable 1 sun illumination power density ( $100 \text{ mW/cm}^2$ ). An aqueous solution of  $0.2 \text{ M H}_2\text{SO}_4$  (measured  $\text{pH} = 0.35$ ) was used as an electrolyte. The  $j - V$  curves were recorded in the dark, under constant illumination and with the chopped light at a chopping frequency of  $\sim 1 \text{ Hz}$ . The applied voltage was scanned at  $50 \text{ mV/s}$  from a Zahner Zennium potentiostat. The measured potential vs Ag/AgCl reference electrode was converted to the reversible hydrogen electrode (RHE) using the eq. 2:

$$E_{RHE} = E_{Ag/AgCl} + 0.197 + 0.059 \text{ pH} \quad (2)$$

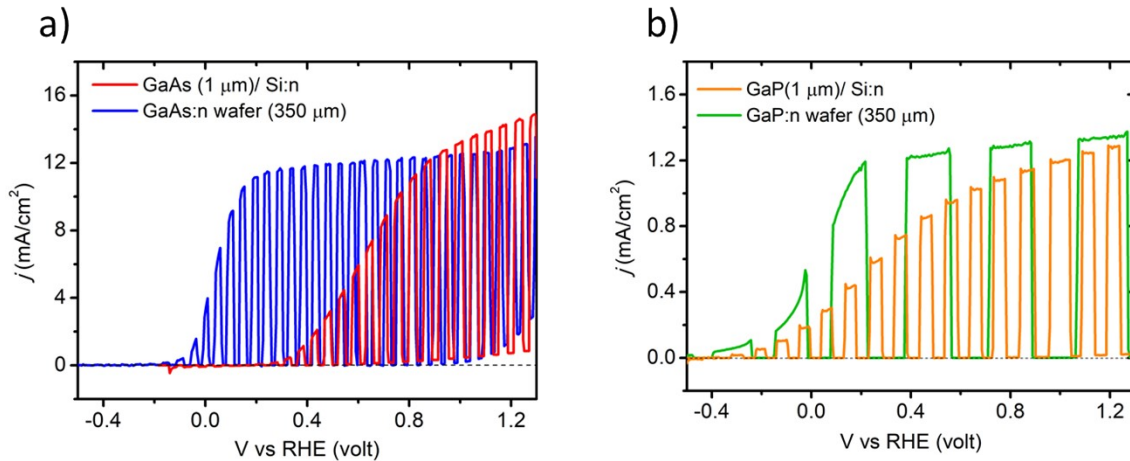


Figure S 6. Photocurrent density vs applied voltage ( $j - V$ ) curves measured under 1-sun illumination in  $0.2 \text{ M H}_2\text{SO}_4$  for the commercial  $350 \mu\text{m}$ -thick GaAs (a), GaP (b) wafer in comparison with the  $1 \mu\text{m}$ -thick  $\text{GaP}_{1-x}\text{As}_x$  with  $x(\text{As}) = 1$  (GaAs) and  $x(\text{As}) = 0$  (GaP) grown on Si substrate.

Apart from the results already shown and discussed in the main file, the evolution of the net photocurrent and experimental and theoretical bandgaps were determined as a function of the As content, and are given in Figure S7.

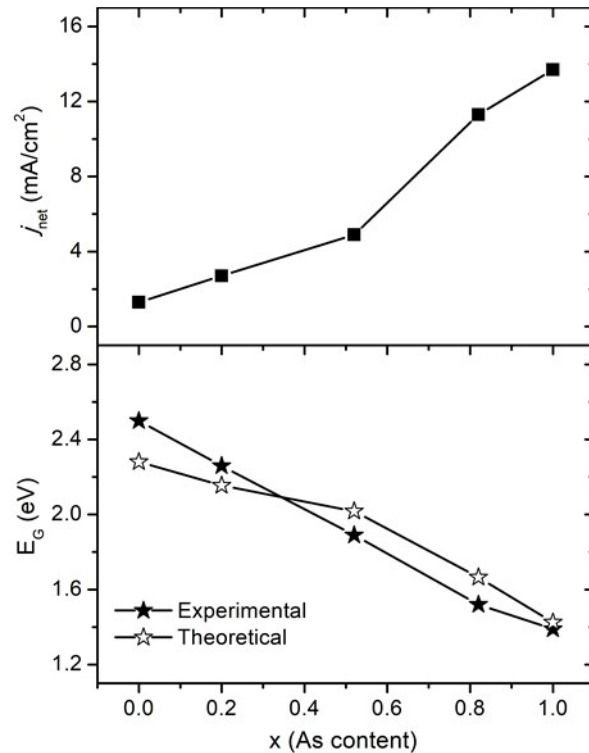


Figure S 7. Variation of the net photocurrent density ( $j_{\text{net}} = j_{\text{light}} - j_{\text{dark}}$ ) at 1.23 V and the optical bandgap ( $E_G$ ) as a function of  $x(\text{As})$  for  $\text{GaP}_{1-x}\text{As}_x/\text{Si}$ . The experimental bandgap is deduced from the optical constants obtained by ellipsometry, the theoretical bandgap at  $\Gamma$ ,  $X$  and  $L$  valleys is calculated for the  $\text{GaP}_{1-x}\text{As}_x$  alloy as a function of  $x(\text{As})$ .<sup>4</sup>

- 1 T. Quinci, J. Kuyyalil, T.T. Nguyen, Y. Wang, S. Almosni, A. Létoublon, T. Rohel, K. Tavernier, N. Chevalier, O. Dehaese, N. Boudet, J.-F. Béarar, S. Loualiche, J. Even, N. Bertru, A. Le Corre, O. Durand, C. Cornet, Defects limitation in epitaxial GaP on bisterped Si surface using UHVCVD-MBE growth cluster, *Journal of Crystal Growth*. 380 (2013) 157–162. <https://doi.org/10.1016/j.jcrysgro.2013.05.022>.
- 2 I. Lucci, S. Charbonnier, L. Pedesseau, M. Vallet, L. Cerutti, J.-B. Rodriguez, E. Tournié, R. Bernard, A. Létoublon, N. Bertru, A. Le Corre, S. Rennesson, F. Semond, G. Patriarche, L. Largeau, P. Turban, A. Ponchet, C. Cornet, Universal description of III-V/Si epitaxial growth processes, *Phys. Rev. Materials*. 2 (2018) 060401. <https://doi.org/10.1103/PhysRevMaterials.2.060401>.
- 3 D.E. Aspnes, A.A. Studna, Dielectric functions and optical parameters of Si, Ge, GaP, GaAs, GaSb, InP, InAs, and InSb from 1.5 to 6.0 eV, *Phys. Rev. B*. 27 (1983) 985–1009. <https://doi.org/10.1103/PhysRevB.27.985>.
- 4 I. Vurgaftman, J.R. Meyer, L.R. Ram-Mohan, Band parameters for III-V compound semiconductors and their alloys, *Journal of Applied Physics*. 89 (2001) 5815–5875. <https://doi.org/10.1063/1.1368156>.
- 5 A. Hankin, F.E. Bedoya-Lora, J.C. Alexander, A. Regoutz, G.H. Kelsall, Flat band potential determination: avoiding the pitfalls, *J. Mater. Chem. A*. 7 (2019) 26162–26176. <https://doi.org/10.1039/C9TA09569A>.